Transmission System Topology Optimization for Large-Scale Offshore Wind Integration

Hakan Ergun, *Student Member, IEEE*, Dirk Van Hertem, *Senior Member, IEEE*, and Ronnie Belmans, *Fellow, IEEE*

***Abstract*—A method to determine the optimal transmission system topology for multiple offshore wind farms is introduced using a rule-based generic algorithm. The methodology is implemented as a software tool determining the best economical and technically feasible offshore transmission solution. The optimization algorithm takes radial, ring shaped, and meshed transmission topologies into consideration. Besides the investments for the offshore grid also new connections or reinforcements in the existing onshore grid are proposed by the algorithm. The developed tool delivers a set of transmission system topologies ranked after their life cycle system costs with their corresponding transmission voltage and technology (HVAC or HVDC), the necessary transmission equipment, and its rating. The optimization results are based on publicly available data. The achieved results are compared with other studies and validated. The developed tool can be used in the planning phase as a guidance for offshore developers with investment decisions and for long-term offshore grid planning, e.g., towards an offshore supergrid.**

***Index Terms*—HVDC, offshore grid topology, offshore wind, optimization, transmission system investments.**

I. Introduction

THE European Union has set ambitious goals regarding CO_2 reduction and integration of renewable energy sources. By 2020, 20% of the European energy supplied should be from renewable sources with 20% CO_2 emission reduction compared to the value of 1990 and an increase in energy efficiency with 20% compared to business as usual. By 2050, the CO_2 reduction should reach 80%–95%, resulting in nearly 100% electricity generation from renewables [1]. To achieve these goals, large-scale integration of renewable energy sources is indispensible. Wind farms with high power ratings are expected to supply a significant portion of future energy. In offshore areas, higher and more constant wind speeds and higher utilization offer an opportunity for large-scale integration of renewable generation. Another argument in favor of large-scale offshore wind integration is the low direct visual and environmental impact compared to onshore. Large rotor diameters and higher towers of onshore wind farms decrease their social acceptance for large-scale integration.

In order to utilize the offshore energy, new transmission investments are needed. These new transmission assets are long-term and costly investments, which must be planned very carefully. Especially offshore, the construction of transmission systems requires high investments. Nevertheless, it is important for a grid planner to consider not only the cheapest solution, but also to compare it with potential alternatives having other advantages than merely lowest costs.

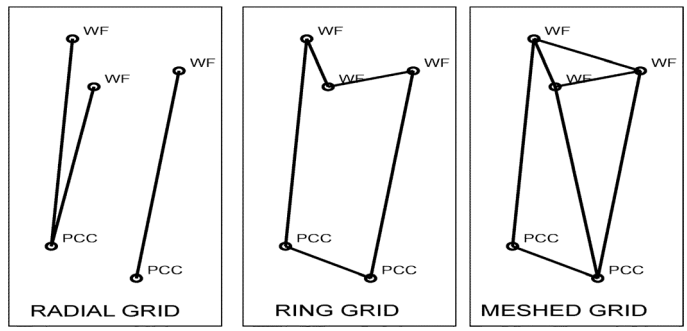

Fig. 1. Different grid topologies.

Existing offshore wind farms, often near-shore or at a relative short distance from shore, are connected radially to the main electricity grid. Wind farms at larger distances from shore and with higher power ratings are under development. For the connection of wind farms, an integrated approach, considering not only single connections, can help to optimize the investments in the offshore transmission system. Ring shaped, clustering of wind farms, or meshed grids can be more economic than single radial connections (Fig. 1). Therefore, different possibilities to connect multiple offshore wind farms should be analyzed to determine the best connection topology.

Optimal connection topologies within offshore wind farms is a well-known topic [2]–[5]. As offshore wind farms have been built as individual projects, so far there are only a few studies on optimal offshore transmission topologies. Some studies on optimal transmission schemes use genetic algorithms [6] for single, specific projects. Such algorithms mostly consider the connection of two wind farms to a single given point of common coupling (PCC). The optimization uses a set of predefined transmission topologies to find the best solution consisting of different technologies (HVAC and HVDC).

The proposed algorithm aims to optimize the transmission topology[1] with a higher degree of freedom. With this approach, each offshore wind farm and PCC can be connected to another wind farm and/or a PCC either with HVAC or HVDC technology. In this way, the number of possible topologies increases. In order to keep the computations limited, a search algorithm is

Manuscript received August 29, 2011; revised February 14, 2012; accepted May 08, 2012. Date of publication June 12, 2012; date of current version September 14, 2012.

The authors are with the Department of Electrical Engineering (ESAT/ELECTA), University of Leuven (KU Leuven), 3001 Heverlee, Belgium (e-mail: hakan.ergun@esat.kuleuven.be; dirk.vanhertem@esat.kuleuven.be; ronnie.belmans@esat.kuleuven.be).

Digital Object Identifier 10.1109/TSTE.2012.2199341

[1]In this paper, the topology describes the connections between nodes and the technologies that each path uses.

implemented in a generic tool, using rule-based investment decisions. The tool can be used to analyze arbitrary projects as all input data such as locations of the wind farms and the possible PCCs can be user defined. This way also the connection of wind farms to PCCs in multiple countries can be analyzed.

In order to maintain accuracy, the optimization algorithm takes besides investment costs, also costs for losses, maintenance, and nonharvested energy into account. The optimization algorithm is implemented as a software tool using Matlab. The power flow and optimal power flow calculations during the optimization process are performed using Matpower [7].

The paper is organized as follows: Section II gives the description of the optimization problem. In Section III, the optimization algorithm is explained. Section IV shows the cost functions used and their validation. In Section V, results achieved with the software tool are shown and compared to other study cases. In Section VI, conclusions are drawn and suggestions for future work are given.

II. Optimization Problem

The main goal of the developed algorithm is to find the best economical transmission solution which fulfills all technical constraints. The optimal solution is determined by minimizing the life cycle system costs, including the investments, losses, maintenance, and nonharvested energy due to unavailability during the lifetime of the transmission system. The objective function is the sum of these costs over the lifetime (1), which has to be minimized. The index i symbolizes annual costs

$$C_{\mathrm{lcsc}} = C_{\mathrm{inv}} + \sum_{i=1}^{\mathrm{lifetime}} (C_{\mathrm{loss},i} + C_{\mathrm{main},i} + C_{\mathrm{nte},i}). \quad (1)$$

The variables taken into account during the optimization are geometry of the transmission system, transmission technology for each path, and the voltage level of the transmission system, where for HVAC and HVDC different voltage levels exist. The optimization variables are limited by given voltage respectively current ratings.

In addition to limitations of optimization variables, the system constraints must be respected. First, the power flow equations have to be fulfilled. In this work, an ac power flow method is used to calculate equipment ratings, because submarine cables have much higher capacitances compared to overhead lines so that the effect of the reactive power on the voltage magnitude cannot be neglected. The power flow equations are given in (2a)–(2e), where $\underline{\mathbf{Y}}$ is the admittance matrix of the system, P_i and Q_i are, respectively, the active reactive power injections in node i, and $\underline{\mathbf{U}}$ is a matrix with the complex voltages of each node in the main diagonal [8]. The admittance matrix of the system depends on the optimization variables and has to be updated with the optimization variables

$$\mathbf{0} = 3\underline{\mathbf{U}}\underline{\mathbf{Y}}^*\underline{\mathbf{u}}^* - (\mathbf{p} + j\mathbf{q}) \quad (2a)$$

with

$$\underline{\mathbf{U}} = \mathrm{diag}(\underline{U}_1\underline{U}_2 \ldots \underline{U}_N) \quad (2b)$$

$$\underline{\mathbf{u}} = [\underline{U}_1\underline{U}_2 \ldots \underline{U}_N]^T \quad (2c)$$

$$\mathbf{p} = [P_1 P_2 \ldots P_N]^T \quad (2d)$$

A. Define input data
B. Create starting topologies → determine best voltage level, transmission technology and equipment ratings
C. Create new topologies with GA → determine best voltage level, transmission technology and equipment ratings
D. Save and rank all feasible results

Fig. 2. Working principle of the developed algorithm.

with

$$[Q_1 Q_2 \ldots Q_N]^T. \quad (2e)$$

Additional constraints relate to the points of common coupling and voltage limits in each node. The amount of power injected in the available points of common coupling ($\mathbf{P}_{\mathrm{inj}}$) may not exceed the limits ($\mathbf{P}_{\mathrm{max}}$) set by the TSO in order to secure stable operation of the main grid (3a). Additionally, the magnitude of the voltage in each node must be between the set voltage limits (3b)

$$\mathbf{P}_{\mathrm{inj}} \leq \mathbf{P}_{\mathrm{max}} \quad (3a)$$

$$U_{\mathrm{min}} \leq |\underline{\mathbf{U}}| \leq U_{\mathrm{max}}. \quad (3b)$$

The functions used for the loss calculation, the current ratings of the cables, and the costs are nonlinear and discontinuous.[2] As such, the optimization problem is nonconvex and cannot be solved easily. Different solvers from different software packages have been tested with no success of correctly solving the optimization problem. Therefore, an intelligent algorithm has been developed, which is explained in detail in Section III.

III. Optimization Algorithm

If every wind farm and PCC can be connected to another wind farm or PCC, for a small number of wind farms and PCCs, all possible topologies can be enumerated and the transmission voltage and technology optimized using brute force. This approach cannot be applied to case studies with larger numbers of wind farms because the number of possible topologies increases exponentially with the number of nodes.

To determine the optimal topology, technology, voltage level, and equipment ratings, the optimization algorithm is developed (Fig. 2). In the algorithm, first input data is defined to specify case studies. After specification of the case study, a set of starting topologies is created as described in Section III-B. New topologies are created based on these starting topologies using a self-developed genetic algorithm. For each topology created, the voltage level, the transmission technology, and the equipment ratings of the related components are optimized deterministically, using the algorithm described in Section III-E. At the end of the algorithm, all feasible solutions are saved and ranked in terms of life cycle system costs. Ranking of the outcomes gives the user the possibility to compare different candidate solutions, even those that come at a higher cost (e.g., comparing ac and dc solutions).

[2]E.g., when the voltage level of the offshore transmission system is the same as the voltage level of the existing system, transformers would be unnecessary and have zero costs and losses.

Wind farms	**Points of common coupling**
• Geometric coordinates • Rated power • Collection grid voltage • Equivalent full load hours	• Geometric coordinates • Maximum power to be injected • Voltage level
Economical Data	**Other Data**
• Energy price • Expected lifetime • Interest rate • Cost data (optional)	• Geometric coordinates of onshore areas • Geometric coordinates of prohibited areas • Maximum power per transmission path

Fig. 3. Input data for the optimization.

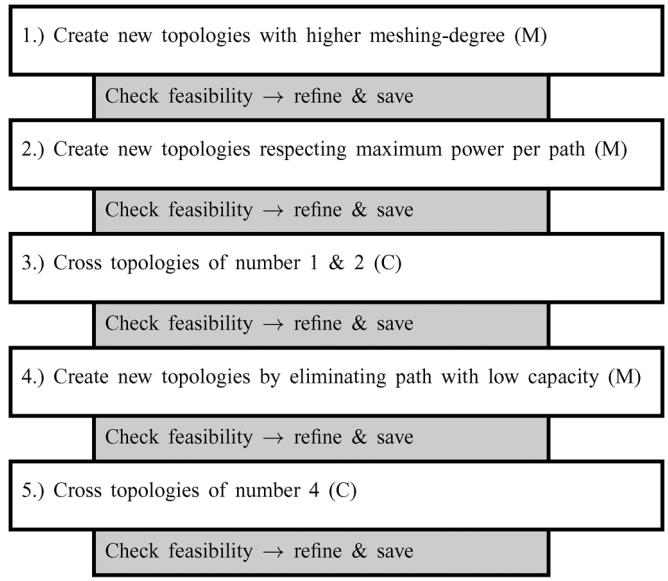

Fig. 4. Working principle of genetic algorithm with embedded algorithm for optimizing transmission voltage, transmission technology, and equipment ratings; (M) states modification, (C) states crossing.

A. Data Initialization

Fig. 3 shows the required input data for the optimization algorithm to specify a case study.

A set of cost data and power system component properties are stored in an independent database. The data in this database are obtained from public sources, and can easily be altered using self-defined input data (e.g., data obtained from manufacturers).

B. Definition of Starting Topologies

A number of starting topologies are defined, to be modified during the optimization process. Two different sets of starting topologies are used in the algorithm. The first set consists of ring-shaped topologies where wind farms and PCCs are connected to the nearest wind farms or PCCs (Fig. 1). In order to guarantee that this approach does not end in a single solution, the starting point of the ring is varied. To increase the variety of starting topologies, partially random topologies are derived from the ring-shaped ones. Therefore, short connection paths are kept and long connection paths are replaced by randomly chosen new connection paths.

The second set of starting topologies is radial. In these starting cases, every wind farm is connected separately to a PCC onshore, where the wind farms are distributed among all PCCs taking into account the maximum amount of power, which can be injected in these PCCs.

For all starting topologies, the transmission voltage, transmission technology, and equipment ratings are optimized using the subalgorithm as described in Section III-E, called "refiner" throughout the following paragraphs.

C. Creation of New Topologies Using a Genetic Algorithm

A genetic algorithm is used to create new sets of topologies, applied to all starting topologies, in order to obtain lower lifetime system costs. Using the "refiner," the best transmission voltage, transmission technology, and transmission equipment ratings are calculated for each topology obtained with the genetic algorithm. A flowchart of the genetic algorithm with the embedded "refiner" is depicted in Fig. 4.

For the next generation of topologies, each node of the transmission system is connected to at least two different nodes. This way, transmission systems with a higher degree of meshing are created. The feasibility of each new topology is checked using the transmission voltage and equipment ratings of the corresponding starting topology (parent topology). Therefore, a power flow calculation with Matpower [7] is performed, where with the convergence of the calculation, a decision about the feasibility of the topology is made. If the power flow calculation converges, the topology is investigated further with the "refiner" and saved, else the topology is discarded.

In the next step, all topologies are modified, so that the power flow on a single connection path cannot exceed a maximum value as defined in the input data set. This limit can be given by the TSO in order to maintain system security or can be/is derived from technological or geographical constraints. The limitation of the maximum power flow is done by iteratively adding new connection paths to the system. Topologies obtained this way are checked for feasibility as explained above and the refiner is applied to feasible topologies, whereas unfeasible topologies are discarded.

In order to find better transmission system topologies, the obtained topologies are crossed with each other using the subalgorithm described in Section III-D.

A major part of investment costs is caused by the installation of equipment. If there are connection paths with low power ratings, the installation costs can be much higher than the equipment costs themselves. To avoid such cases, connection parts with low transmission capacities are eliminated sequentially in the last part of the genetic algorithm. The threshold for the minimum amount of transmittable power can be defined by the user. Each new topology is checked for feasibility and refined and saved if feasible. Topologies obtained this way are crossed with each other, using the subalgorithm as described in Section III-D.

D. Crossing Topologies

In this subalgorithm, topologies delivering the lowest costs are crossed with each other in order to find better topologies. With the software used, every topology is coded as a symmetrical incidence matrix with size $(N \times N)$, where N is the number

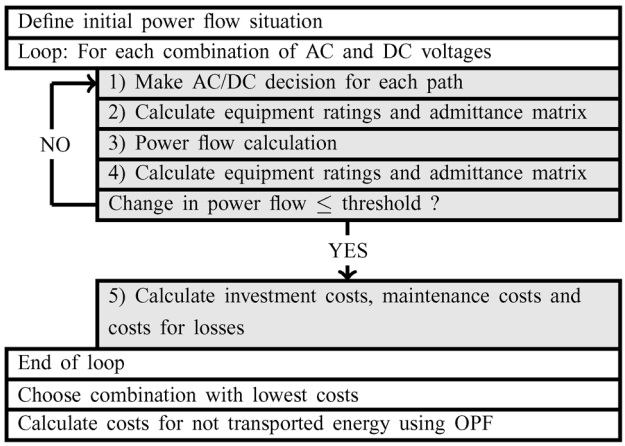

Fig. 5. Flowchart of algorithm for optimizing voltage level, transmission technology, and equipment ratings.

of nodes. A 1 at position (i, j) indicates that node i is connected to node j.

The crossing of different topologies is done using two approaches. In the first one, topologies with a minimum number of connections are created. Therefore, incident matrices of two topologies are multiplied element wise. This way only topologies with common connection paths of two topologies remain, mathematically the intersection of two topologies $(T_1 \cap T_2)$.

The second approach aims to create topologies with a higher number of connection paths. This is done by adding incidence matrices of two topologies. That way topologies are created, which consist of all connection paths of both topologies. Mathematically, this is a union set of both connection topologies $(T_1 \cup T_2)$.

E. Optimization of Transmission Technology and Voltage

Within this subalgorithm, the voltage level, the transmission technology of each path, and the ratings of equipment used are optimized for given topologies. The principle of this algorithm is illustrated in Fig. 5. For the calculation of power flows and equipment ratings, the rated power of the wind farms is taken into account; i.e., the proposed transmission system is able to transfer the maximum wind power to shore.

In the beginning, neither the power flows on the connection paths nor the voltage level of the transmission system are known. Therefore, an initial power flow situation is defined first, based on the topology and the rated power output of the wind farms. Using this initial power flow, the investment costs, the maintenance costs, and the costs of losses are calculated for all possible combinations of ac $(U_{\mathrm{AC}} \in \{30\ \mathrm{kV}, 70\ \mathrm{kV}, 150\ \mathrm{kV}, 220\ \mathrm{kV}, 400\ \mathrm{kV}\})$ and dc $(U_{\mathrm{DC}} \in \{\pm 80\ \mathrm{kV}, \pm 150\ \mathrm{kV}, \pm 320\ \mathrm{kV}\})$ voltages in two nested loops. Hence 15 different costs are calculated, whereas the solution with the lowest costs is chosen to be the best. The calculation procedure is described in the following paragraphs.[3]

1) For every combination of possible voltages (e.g., 70-kV ac and ±80-kV dc), the transmission technology of each path is chosen, based on the empirical formula (4) derived from [9]. This decision formula states the break-even distance of HVDC technology for the assumed power flow P_N on each path. As possible dc technology only VSC HVDC is considered[4]

$$l_{\mathrm{DC}} = \max\left\{40, \min\left\{200, 832.5 \cdot P_N^{-0.4}\right\}\right\} \quad (4a)$$

$$l_{\mathrm{offshore}} > l_{\mathrm{DC}} \rightarrow \mathrm{DC\ connection} \quad (4b)$$

$$l_{\mathrm{offshore}} \leq l_{\mathrm{DC}} \rightarrow \mathrm{AC\ connection}. \quad (4c)$$

2) Using the combination of voltage levels and the initially assumed power flow, equipment ratings and sequentially the admittance matrix of the power system are calculated. For the calculation of the admittance matrix, the cable cross-sections have to be determined iteratively. Therefore, it is assumed that the highest available cross-section is used for cables (e.g., obtained from [11] and [12]). Using the current rating of these cables, the minimum number of cables is calculated. Then the minimum cross-section for the minimum number of cables is determined. During the calculation, the charging current of ac cables, which influences the design significantly for long distances and high voltages, is taken into account.
3) With the obtained admittance matrix, a power flow calculation is performed using Matpower [7]. In order to comply with the Matpower data structure, a new function is written, so that depending on the voltage level and the decision for ac or dc, the input data structure is created automatically with all required equipment, such as transformers, cables, and possible HVDC converters included. For the power flow calculation, HVDC converters are modeled as voltage sources behind a reactance [13]. In steady state, the VSCs with voltage control can be presented as PV nodes and VSCs with reactive power control as PQ nodes behind a reactance. As Matpower cannot deal with islanded transmission systems, an islanding detection algorithm is written. If islanded grids are detected, the grid is divided into subgrids and the power flow calculation is performed separately for these subgrids.
4) The result of the power flow calculation is based on an admittance matrix, calculated with preliminary initialized values. Therefore, a new admittance matrix and equipment ratings based on the actual power flow results are calculated. This procedure is repeated from the ac/dc decision (as the ac/dc decision is based on the power flow on each path), until the change in power flows is lower than a threshold or a maximum number of iterations is reached.
5) Life cycle costs of the transmission system are calculated after the iterative power flow calculations using data obtained from the last iteration. For the cost-calculation, the costs for investment, maintenance, and losses are considered. To calculate the transmission losses accurately, the power output of wind farms is modeled with a resolution of one hour. Therefore, a random series of Weibull distributed wind speeds is generated. This series is applied to a wind power output curve of a known wind farm, similar to curves in [14].

[3]Numbers 1–5 in the text indicate blocks 1–5 in Fig. 5.

[4]In this work, LCC HVDC technology is not taken into consideration because of large reactive power demands, the big filter installations, and the inability to produce an independent rotating electrical field to connect a weak offshore grid. These factors make LCC technology less suitable for offshore applications [10].

Using the above described procedure, 15 values for the life cycle system costs are retained for possible combinations of ac and dc voltage levels. To be more accurate, the nonharvested energy should be taken into account for all 15 combinations. But as the calculation of the nonharvested energy is based on optimal power flow (OPF), and therefore, is time intensive, it is only performed for the combination with the lowest sum of investment, maintenance and loss costs

$$\min\left\{C_{\text{inv}} + \sum_{i=1}^{\text{lifetime}} \left(C_{\text{loss},i} + C_{\text{main},i}\right)\right\}. \tag{5}$$

The same time series of output powers is used to calculate the nonharvested energy. Therefore, the duration curve of output power is divided in 11 sections ($P_{\text{out}} = 0\% - 10\%, 10\% - 20\%, \ldots, 90\% - 100\%$) and the probabilities of occurrence of these sections is determined. The nonharvested energy is calculated from

$$W_{\text{NH}} = 8760\ h \cdot \sum_{i=1}^{11} p_i \cdot P_{\text{GL},i} \tag{6}$$

with p_i the probability of power outputs and $P_{\text{GL},i}$ the generation loss in case of these power outputs. The nonharvested energy is converted into costs using the energy price (€/MWh) defined in the input data set.

The wind energy loss for different power outputs ($P_{\text{GL},i}$) is determined using the OPF tool of Matpower by deactivating elements in the transmission system, such as cables, converters, or transformers separately. For the OPF, the generation costs of offshore wind farms is set much lower than equivalent generators onshore, so that the dispatch of offshore wind power with maximal use of offshore wind power is enforced. After running the OPF, the amount of generation loss in case of failure of one element ($P_{\text{GL},j}$) can be determined. The loss of power through wind curtailment is the sum of lost power due to outages of single elements ($P_{\text{GL},j}$) multiplied with the probability of failure (p_j) of these and this for all elements (N_e) in the transmission system

$$P_{\text{GL},i} = \sum_{j=1}^{N_e} p_j \cdot P_{\text{GL},j}. \tag{7}$$

IV. Used Cost Functions and Their Validation

The life cycle costs consist largely of transmission equipment investments. Therefore, the use of reliable and accurate cost data is very important for the outcome of the optimization. The cost functions used in this paper are given in Appendixes A–E. They are derived from publicly available data, obtained from several publications [15]–[23]. In the developed software tool, any alternative cost function can be provided by the user to adapt to different market or geographical conditions.

A. Validation of Cost Functions

In [24], a detailed analysis of investment costs for "round 3" offshore wind farms in the U.K. is given. These investment costs do not include maintenance and losses but do include contingency costs. Cost functions given in the appendix are applied to two case studies and compared to the costs in [24] for validation.

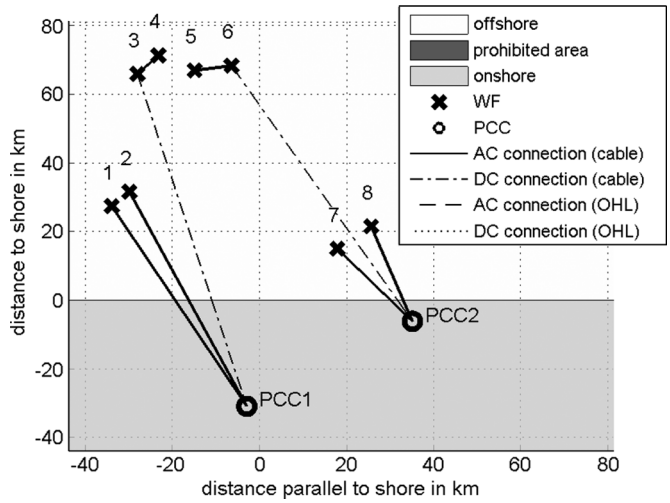

Fig. 6. Case study 1 consisting of eight offshore wind farms and two possible PCCs [24].

Case study 1 (CS1) as depicted in Fig. 6 consists of eight offshore wind farms with a rated power of 550 MW each. There are two possible PCCs and onshore connections are realized with underground cables. The connections between the wind farm clusters (3,4) and (5,6) are realized with 245-kV ac cables.

Using the developed tool,[5] total costs of 2067 M€ are calculated for the given topology, technology, and voltage levels. In [24], costs of 2160 M€ are calculated, where the costs for nonharvested energy are not included. These costs differ approximately 4.5%.

Case study 2 (CS2) consists of 20 wind farms with a rated power of 550 MW each and four possible connection points onshore (PCC). The total transmission system costs of this project amounts to 7460 M€ according to [24]. The results in the optimization tool are determined, using the same topologies, technologies, and voltage levels amount to 7163 M€. In this case, the difference between the both results is 4.1%.

V. Optimization Results

A. Examples of "U.K. Round 3" Study

In this section, the results achieved with the developed algorithm are shown. The results are given for case study (CS1) given in Fig. 6. The main assumptions for the optimization are summarized in Table I.

The optimal topology obtained with the developed algorithm is shown in Fig. 7. The obtained voltage level for this case is 400-kV ac. The optimal technology of each path is chosen to be in HVAC, as the offshore distance is below 30 km for wind farms 1 and 7, connected to PCC 1 and WF 8, connected to PCC 2. Also the distances between WF 2 and WF 3, respectively WF 6 and WF 8, let the algorithm decide in favor of HVAC.

[5]Note that in this case, data and calculation methodology of the tool are used, but not the grid optimization algorithm (starting point is a given topology).

TABLE I
ASSUMPTIONS FOR THE OPTIMIZATION

voltage level of PCCs	$400\ kV$
capacity of PCC1	$2.2\ GW$
capacity of PCC2	$2.2\ GW$
maximum power on one path	$2.2\ GW$
onshore connections	$cabling$
electricity price	$40\ €/MWh$
interest rate	$5\ \%$
full load hours	$3750\ h/a$
lifetime	$20\ ae$

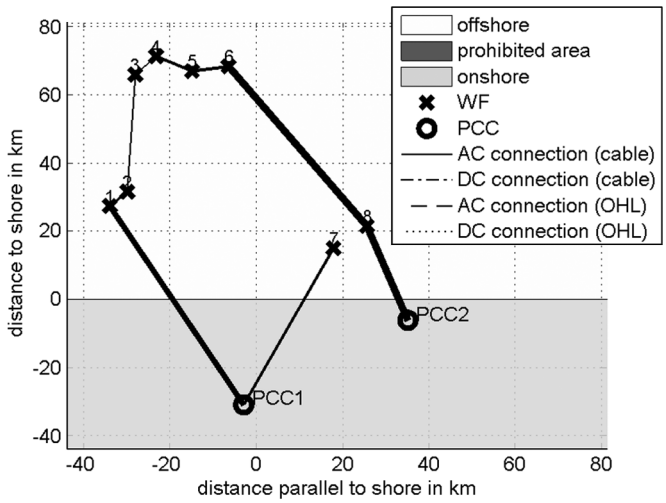

Fig. 7. Optimal topology for case study 1. The thickness of the line indicates the number of parallel circuits/cables.

The total costs during the lifetime of the system are calculated as 1700 M€. This value also includes the costs for nonharvested energy due to unavailability of transmission equipment, with a share of 3.4% of the total system costs for this topology. The costs for the transmission losses during the lifetime equal 6.58% of the total system costs. The determined costs after the optimization are 460 M€, respectively 21% lower than in [24].

Because 400-kV three-core submarine HVAC cables are still under development, the optimization algorithm is also run excluding 400 kV as a possible ac voltage. The optimal topology for this case is shown in Fig. 8, which differs significantly from the proposed topology in the case with 400-kV HVAC. The optimal transmission voltage is 220 kV and the total cost is 1880 M€. Because the voltage is limited to 220 kV, the number of parallel circuits in most corridors increases. The costs for nonharvested energy are 2.9% of the total costs and the costs for transmission losses equal 7.9% of the total costs. With this optimization, cost savings of 280 M€, respectively 13% to the value given in [24] are achieved.

B. Fictive Case With a Forbidden Zone

The optimization results for a fictive case study with longer transmission distances and higher power ratings are shown in Fig. 9. The case consists of three offshore wind farms, with a rated power of 500 MW each. The energy generated by the wind farms can be injected in three PCCs, situated around a fictive city. As a restriction, no cable or overhead line connections

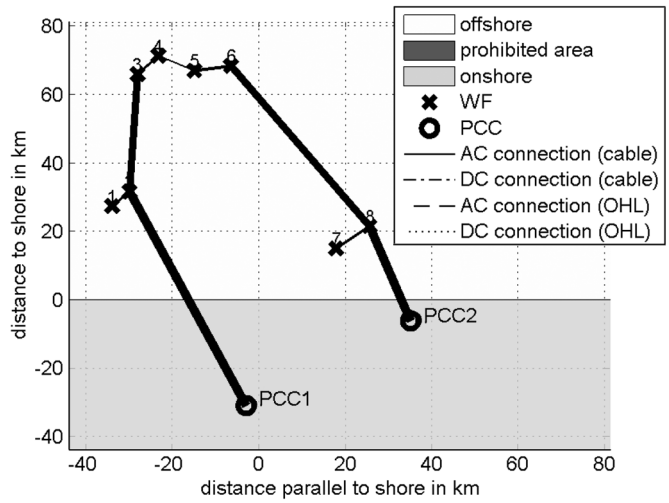

Fig. 8. Optimal topology for case study 1 with exclusion of 400-kV HVAC. The thickness of the line indicates the number of parallel circuits/cables.

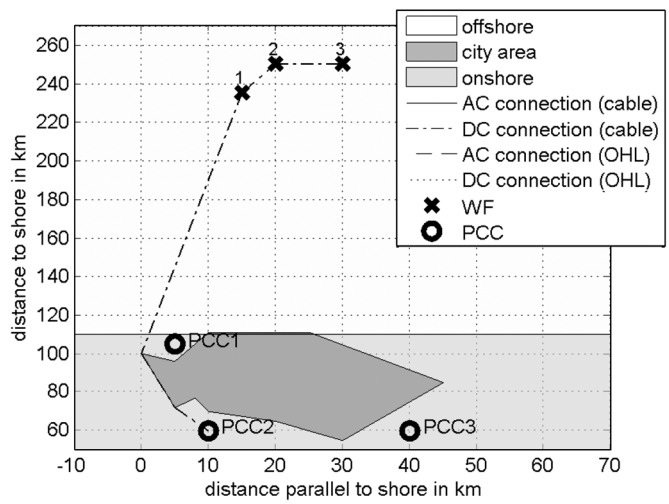

Fig. 9. Optimal topology for the fictive case study.

may be made within the city area. Fig. 9 depicts the results of the optimization using the input data as listed in Table II in addition to the geographical coordinates of the WFs, the PCCs, and the city area. In this case, the optimal transmission system is a multiterminal HVDC system, where the three WFs are connected in series with PCC 2. The optimal transmission voltage is chosen to be ± 320 kV and one system of HVDC cables with different cross sections (500 mm^2, 1400 mm^2, 2800 mm^2) are used for the HVDC connections. In total, 153.6 km of offshore and 51.5 km of onshore cables for the connection of the wind farms are proposed. The total life cycle system costs are calculated to be 1059 M€.

Fig. 10 shows the optimization results, with the capacity of PCC 2 set to 800 MW. In this case, the wind farms are connected first to PCC 1, where 800 MW is injected into the power system. For the remaining 700 MW that needs to be injected into the network, a grid reinforcement between PCC 1 and PCC 2 is proposed, consisting of one system of 400-kV ac cables (three single core cables). In this case, the total life cycle system costs

TABLE II
ASSUMPTIONS MADE FOR THE FICTIVE CASE STUDY

voltage level of PCCs	$400\ kV$
capacity of PCC1	$800\ MW$
capacity of PCC2	$2\ GW$
capacity of PCC3	$800\ MW$
maximum power on one path	$2.2\ GW$
onshore connections	$cabling$
electricity price	$50\ €/MWh$
interest rate	$5\ \%$
full load hours	$4500\ h/a$
lifetime	$25\ ae$

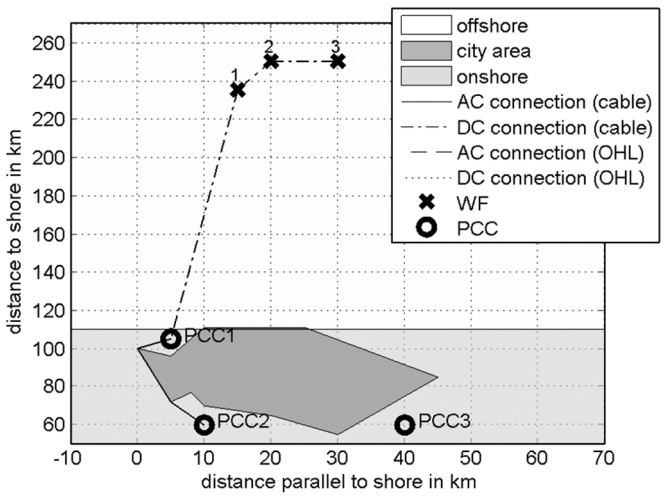

Fig. 10. Optimal topology for the fictive case study showing grid reinforcements.

are determined to be 1074 M€. The proposed voltage of the HVDC connections is ±320 kV, as in the previous case.

C. Computational Efficiency

Fig. 11 shows the evolution of a selected starting topology for the case study CS1 as illustrated in Figs. 6–8, M indicating a modification and C a crossing according to Fig. 4. It can be seen that the best solution for the shown starting topology is reached in the eighth generation. In this particular case, the best solution is obtained from the second offspring of the starting topology only with modifications and no crossings. In general it can be seen that crossings can result in solutions with higher or lower total system costs, whereas modifications result in lower total system costs. The reason is that the modifications are biased to achieve results with lower system costs. During crossings two topologies are merged unbiased in order to increase the variety of topologies. In these cases, system costs of new topologies can be higher or lower than those of their parents.

For the shown case study with six nodes (Figs. 9 and 10), 32 647 possible topologies exist. The optimization algorithm finds the proposed solutions by calculating 1685, respectively 1442, different topologies depending on the assumptions made. More than $3.5 \cdot 10^{13}$ possible topologies exist for the case study (CS1) with 10 nodes, where the solution is found after calculating 3278 different topologies. This shows that the rule-based algorithm finds the solution more effectively in large systems.

The computation time of the case study with six nodes (Figs. 9 and 10) is 3 h 2 min, respectively 2 h 5 min, depending on the

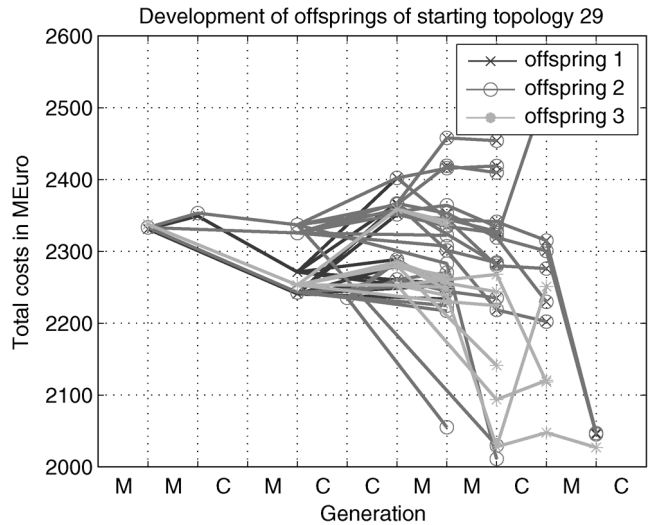

Fig. 11. Evolution of the starting topology.

assumptions made for the grid capacity, whereas 11 h 55 min is required for the case study with 10 nodes. In this time frame, a set of solutions is provided which allow the grid planner to select the most appropriate solution(s) for detailed study.

VI. CONCLUSION

An optimization algorithm for offshore transmission grid development based on an intelligent algorithm was shown. The method uses a set of rules in combination with a self-developed genetic algorithm. The algorithm is implemented in a software tool. The tool is intended to be used by both grid planners and offshore wind developers. The developed tool can solve transmission expansion problems for integrating renewable energy sources into the electricity system offshore as well as onshore with a minimum requirement of input data.

The methodology uses an intelligent multistep decision process. Both ac and dc technologies are considered for both radial and meshed layouts. For the system, the loss due to non-harvested energy as well as the electrical losses are taken into account. The investments take all components into account, including transformers, substations, reactive power compensation, etc. Cost data available from public sources has been used to obtain realistic investment costs. Based on this publicly available data, cost functions have been derived.

The tool has been validated against existing studies, resulting in only minor differences. It has been shown that solutions with lower total investment costs can be found. Results achieved with the tool show that the transmission technology and the used transmission voltage affect the topology of the transmission system. It is shown that starting from a topology through intelligent modifications and crossings, better solutions can be achieved. As the objective of the optimization is the minimization of total system costs, the used cost functions play an important role.

The methodology developed can be applied to offshore grid extension as well as be extended to general transmission system expansion, for example towards a supergrid. The computational performance of the used algorithm or the implementation has

TABLE III
COST COEFFICIENTS FOR AC OFFSHORE CABLES FOR DIFFERENT VOLTAGE LEVELS [15], [23]

	30 kV	70 kV	150 kV	220 kV	400 kV
A	0.411	0.688	1.971	3.181	5.8038
B	0.596	0.625	0.209	0.11	0.044525
C	0.041	0.0205	0.0166	0.0116	0.0072
D	$17 \cdot 10^4$				
E	8.98				

TABLE IV
COST COEFFICIENTS FOR AC ONSHORE CABLES FOR DIFFERENT VOLTAGE LEVELS AND NUMBER OF SYSTEMS [18]

Voltage levels	$\leq$ 150 kV		220 kV		400 kV	
Nr. of systems	1	2	1	2	1	2
B	265	530	385	770	750	1500
C	300	450	400	600	500	750

to be improved to apply the developed methodology to larger power systems.

APPENDIX A
COSTS FOR AC CABLES AND OVERHEAD LINES

There are three major factors related to the costs of ac submarine cables. The first factor is the current rating of the cable, determined by the cross section and relates to the amount of copper (or aluminum) used in the cable. The second one is the rated voltage of the cable, which determines the insulation material. The item, having the highest uncertainty is the cable installation cost. The used investment cost functions for different voltages and power ratings are shown in (8a), where n is the number of cables, l_{offshore} the offshore cable length in kilometers and S the rated apparent power in MVA [23]. The coefficients A, B, C, D, and E for different voltage levels are given in Table III. These functions include both investment and installation costs

$$C_{\text{ac,sub}} = \frac{(A + Be^{C \cdot S} + D) \cdot (9n + 1)}{10E} \cdot l_{\text{offshore}} \; [€]. \quad (8a)$$

The cost function used for onshore cables is given in (8b), where A is the cross section of cables in millimeters squared. This function includes installation costs (coefficient C). The coefficients B and C for different voltage levels and number of systems are given in Table IV.

Besides the investment and installation costs, also the costs for losses and nonharvested energy have to be taken into account. The losses can be determined using the resistance of the cable. During the determination of losses in an ac cable system, the losses due to charging currents should not be neglected. For the calculation of the nonharvested energy, the unavailability of cables must be known. Several publications [16], [25]–[29] have been analyzed and an unavailability of $21 \cdot 10^{-4}/(\text{km} \cdot \text{a})$ has been chosen with a mean repair time of 30 days[6] for submarine cables and 10 days for underground cables. Another cost component is the maintenance costs, where for submarine and underground cables 200 k€/a per cable system are assumed based on [16]

$$C_{\text{ac,land}} = B \cdot \left(0.75 + 0.25\frac{A}{1400}\right) + C \; [\text{k€/km}]. \quad (8b)$$

Investment costs for ac overhead lines are determined using (8c), where U_N is the rated voltage in kilovolts, A_{Al} the cross section of aluminum in millimeters squared, and n_b number of wires per bundle [30]. Also in this function the installation costs are included

$$C_{\text{ohl,inv}} = 60 + 0.4 \cdot U_N + 0.4 \cdot \sqrt[4]{n_b} \cdot A_{Al} \; [\text{k€/km}]. \quad (8c)$$

The calculated investment costs $C_{\text{ohl,inv}}$ are valid for OHL systems with two circuits. For systems with another number of circuits, the calculated costs can be multiplied or divided correspondingly. For the unavailability of overhead lines, $0.002 \cdot 10^{-4}/(\text{km} \cdot \text{a})$ and a mean repair time of 4 h are assumed based on [31]. For maintenance costs, 1% of investment costs per year are assumed.

APPENDIX B
TRANSFORMER SUBSTATION COSTS

Due to cost intensive construction of offshore platforms there is a large cost difference between off- and onshore substation costs. The cost functions used for offshore, respectively onshore, transformer substations are given in (9a) and (9b). For the loss calculation of transformers both load and no load losses are taken into account. Typical values for transformer losses can be found in [32]. To determine the nonharvested energy an unavailability factor of $6 \cdot 10^{-3}/\text{a}$ with a mean repair time of 10 days for onshore and 21 days offshore installations is used. For maintenance costs, 0.4% of the investment costs per year are assumed [16]

$$C_{\text{tr,off}} = 120 \cdot 10^3 \cdot \left(\frac{S_{\text{Tr}}}{300}\right)^{-0.413} \; [€/\text{MVA}] \quad (9a)$$

$$C_{\text{tr,on}} = 30 \cdot 10^3 \cdot \left(\frac{S_{\text{Tr}}}{300}\right)^{-0.413} \; [€/\text{MVA}]. \quad (9b)$$

APPENDIX C
COSTS OF COMPENSATION EQUIPMENT

Investment costs of compensation equipment is derived from [15] and [33]. For offshore inductances, investment costs of 10 k€/MVA and 90 k€/MVA for onshore, respectively offshore, are used. For SVCs, investment costs of 60 k€/MVA are assumed. The losses of compensation devices are modeled as given in [34]. For the unavailability and maintenance costs of inductances the same numbers as in case of transformers are used. For SVCs the unavailability and maintenance costs, data of HVDC converters is used.

APPENDIX D
COSTS FOR DC CABLES AND OVERHEAD LINES

As in the case of ac submarine cables, the current rating, the voltage rating, and the installation costs determine the investment costs for dc cables [15], [23]. Equations (10a) and (10b) illustrate investment costs for off- and onshore cables, respectively. Here P is the rated power in W, l_{offshore} and l_{onshore} the offshore, respectively onshore, cable lengths. As the same value for cable prices is used, the only difference between offshore

[6]Predefined values are used, but if the user has better data available, they can easily be inserted into the dataset.

TABLE V
COST COEFFICIENTS DC CABLES FOR DIFFERENT VOLTAGE LEVELS [15], [22], [23]

voltage levels	$\pm 80\ kV$	$\pm 150\ kV$	$\pm 320\ kV$
A	$-0.25179 \cdot 10^6$	$-0.1 \cdot 10^6$	$0.286 \cdot 10^6$
B	0.03198	0.0164	0.00969
D_{off}	$22 \cdot 10^4$		
D_{on}	$5 \cdot 10^4$		
E	8.98		

and onshore cables is the installation cost (D_{off}, respectively, D_{on}). The coefficients A, B, D, and E are given in Table V. For dc overhead lines, the cost function in (8c) is used

$$C_{\text{dc,off}} = \frac{(A + B \cdot P + D_{\text{off}}) \cdot (9n + 1)}{10E} \cdot l_{\text{offshore}}\ [€] \tag{10a}$$

$$C_{\text{dc,on}} = \frac{(A + B \cdot P + D_{\text{on}}) \cdot (9n + 1)}{10E} \cdot l_{\text{onshore}}\ [€]. \tag{10b}$$

The costs of losses are again determined with the ohmic losses and the energy price. In this case, no additional losses due charging occur. For the unavailability and maintenance costs of one pair of dc cables, the same values as for ac cables are used. For the unavailability and maintenance costs of dc overhead lines, the same data as ac overhead lines are used.

APPENDIX E
HVDC CONVERTER STATION COSTS

As in the case of transformer substations, there is a significant difference between off- and onshore HVDC converter station costs, because of the cost intensive offshore installation. There is little information about HVDC converter station costs in the reviewed literature as mentioned in previous subsections. For investment costs, a linear cost function is used (11a) and (11b) for offshore, respectively onshore, converters, where $P_{N,\text{conv}}$ is the rated power of the converter in MW [15], [23]

$$C_{\text{dc,off}} = \left(42 + 27 \cdot \frac{P_{N,\text{conv}}}{300}\right) \cdot 10^6\ [€] \tag{11a}$$

$$C_{\text{dc,on}} = \left(18 + 27 \cdot \frac{P_{N,\text{conv}}}{300}\right) \cdot 10^6\ [€]. \tag{11b}$$

Losses as a function of the utilization of VSC HVDC converters are given in

$$P_{L,\text{conv}} = 0.0042558 \cdot e^{1.1004171 \cdot \text{UF}} \tag{12}$$

with UF as the utilization factor [29]. For the calculation of not transported energy, an unavailability of 0.02/a with a mean repair time of 15 days onshore, respectively 30 days offshore, is used. As maintenance costs 0.5% of investment costs per year are assumed based on [16].

REFERENCES

[1] EU Action Against Climate Change—Leading Global Action to 2020 and Beyond European Commission, Tech. Rep., 2009.

[2] J. Gonzalez, A. Rodriguez, J. Mora, J. Santos, and M. Payan, "A new tool for wind farm optimal design," in *Proc. IEEE Bucharest Power Tech. Conf.*, Bucharest, Romania, 2009, pp. 1338–1348.

[3] H. Lingling, F. Yang, and G. Xiaoming, "Optimization of electrical connection scheme for large offshore wind farm with genetic algorithm," in *Proc. Int. Conf. Sustainable Power Generation and Supply*, Nanjing, China, 2009.

[4] Z. Li, M. Zhao, and Z. Chen, "Efficiency evaluation for offshore wind farms," in *Proc. Int. Conf. Power System Technology*, Chongqing, China, 2006.

[5] M. Banzo and A. Ramos, "Stochastic optimization model for electric power system planning of offshore wind farms," *IEEE Trans. Power Syst.*, vol. 26, no. 3, pp. 1338–1348, Aug. 2010.

[6] M. Zhao, Z. Chen, and F. Blaabjerg, "Optimisation of electrical system for offshore wind farms via genetic algorithm," *IET Renew. Power Generat.*, vol. 3, no. 2, pp. 205–213, 2009.

[7] R. D. Zimmerman and C. E. Murillo-Sanchez, "MATPOWER: Steady-state operations, planning, and analysis tools for power systems research and education," *IEEE Trans. Power Syst.*, vol. 26, no. 1, pp. 12–19, Feb. 2011.

[8] D. Oeding and B. Oswald, *Elektrische Kraftwerke und Netze*, 6th ed. New York: Springer-Verlag, 2004, 3-540-00863-2.

[9] H. Ergun, D. Van Hertem, and R. Belmans, "CoST of wind—Appropriate connection selection tool for offshore wind farms," in *Proc. Int. Workshop on Large-Scale Integration of Wind Power Into Power Systems as Well as on Transmission Networks for Offshore Wind Power Plants*, Quebec, Canada, 2010.

[10] H. Ergun, D. Van Hertem, and R. Belmans, "Multilevel optimization for offshore grid planning," in *Proc. Cigre Int. Symp.—The Electric Power System of the Future*, Bologna, Italy, 2011.

[11] ABB, XLPE Submarine Cable Systems Attachment to XLPE Land Cable Systems-User's Guide 2007, 2nd ed.

[12] ABB high voltage cable unit, HVDC Light Cables-Submarine and Land Power Cables Sweden 2006.

[13] S. Cole, "Steady-State and Dynamic Modelling of VSC HVDC Systems for Power System Simulation," Ph.D. dissertation, Katholieke Universiteit Leuven, Leuven, Belgium, 2010, 978-94-6018-239-6.

[14] B. Hayes, I. Ilie, A. Porpodas, S. Djokic, and G. Chicco, "Equivalent power curve model of a wind farm based on field measurement data," in *Proc. IEEE PowerTech Trondheim*, Jun. 19–23, 2011.

[15] B. Van Eeckhout, D. Van Hertem, M. Reza, K. Srivastava, and R. Belmans, "Economic comparison of VSC HVDC and HVAC as transmission system for a 300 MW offshore wind farm," *Eur. Trans. Elect. Power*, vol. 20, no. 5, pp. 661–671, Jul. 2010.

[16] P. Bresesti, W. Kling, R. Hendriks, and R. Vailati, "HVDC connection of offshore wind farms to the transmission system," *IEEE Trans. Energy Convers.*, vol. 22, no. 1, pp. 37–43, Mar. 2007.

[17] B. Oswald, A. Müller, and M. Krämer, Vergleichende Studie zu Stromübertragungstechniken im Höchstspannungsnetz, For Wind Hannover & Oldenburg, Germany, Tech. Rep., 2005.

[18] H. Brakelmann, Netzverstärkungs-Trassen zur Übertragung von Windenergie: Freileitung oder Kabel? Universität Duisburg-Essen, Tech. Rep., 2004.

[19] B. Wiederkehr, Einheitskosten—Beilage zur Branchenempfehlung Netzbewertung Verband Schweizerischer Elektrizitätsunternehmen VSE, Aarau, Switzerland, Tech. Rep., 2004.

[20] E. D. Stoutenburg and M. Jacobson, "Optimizing offshore transmission links for marine renewable energy farms," in *Proc. Oceans 2010*, Seattle, WA, 2010.

[21] S. Cole, D. Van Hertem, and R. Belmans, "Connecting Belgium and Germany using HVDC: A preliminary study," in *Proc. IEEE Power Tech. Lausanne*, 2007, pp. 1215–1219.

[22] D. Ravemark and B. Normark, Light and invisible—Underground transmission with HVDC Light ABB, 2005.

[23] S. Lundberg, Performance Comparison of Wind Park Configurations Department of Electric Power Engineering—Chalmers University Of Technology, Goteborg, Sweden, Tech. Rep., 2003.

[24] I. Spreeuwenberg, D. Moore, D. Coates, C. Grant, S. Cowdroy, P. Brooks, and Z. Ndlovu, The Crown Estate—Round 3 Offshore Wind Farm Connection Study National Grid & E-connect, Tech. Rep., 2008.

[25] T. Ackermann, N. Barberis Negra, J. Todorovic, and L. Lazaridis, "Evaluation of electrical transmission concepts for large offshore wind farms," in *Proc. Copenhagen Offshore Wind Conf. Exhibiton*, Denmark, 2005.

[26] A. Underbrink, J. Hanson, A. Osterholt, and W. Zimmermann, "Probabilistic reliability calculations for the grid connection of an offshore wind farm," in *Proc. 9th Int. Conf. Probabilistic Methods Applied to Power Systems, KTH*, Stockholm, Sweden, 2006.
[27] M. Nandigam and S. K. Dhali, "Optimal design of an offshore wind farm layout," in *Proc. SPEEDAM—Int. Symp. Power Electronics, Electrical Drives, Automation and Motion*, 2008, pp. 1470–1474.
[28] E. Spahic, A. Underbrink, V. Buchert, J. Hanson, I. Jeromin, and G. Balzer, "Reliability model of large offshore wind farms," in *Proc. IEEE Power Tech. Conf.*, Bucharest, Romania, Jun. 28–Jul. 2, 2009.
[29] B. Railing, G. Moreau, L. Ronstrom, J. Miller, P. Bard, J. Lindberg, and P. Steckley, "Cross sound cable project—Second generation VSC Technology for HVDC," in *Proc. Cigre Session*, Paris, France, 2004.
[30] F. Kiessling, P. Nefzger, and U. Kaintzyk, *Freileitungen*. Heidelberg, Germany: Springer Verlag, 2001, 3-540-42255-2.
[31] M. Obergünner, M. Schwan, C. Krane, K. Von Sengbusch, C. Bock, and D. Quadflieg, Ermittlung von Eingangsdaten für Zuverlässigkeitsberechnungen aus der VDN-Störungsstatistik Jul. 2004.
[32] V. Crastan, *Elektrische Energieversorgung 1*, 2nd ed. Heidelberg, Germany: Springer-Verlag, 2006, 978-3-540-69439-7.
[33] L. Cai, I. Erlich, and G. Stamtsis, "Optimal choice and allocation of FACTS devices in deregulated electricity market using genetic algorithms," in *Proc. IEEE PES Power Syst. Conf. Exposition*, 2004, pp. 201–207.
[34] N. G. Hingorani and L. Gyugyi, *Understanding FACTS*. New York: IEEE Press, 2000, 0-7803-3455-8.

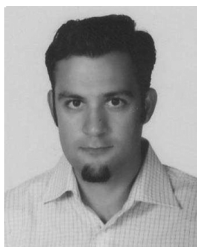

Hakan Ergun (S'10) received the Dipl.-Ing. degree in electrical engineering from the Technical University Graz in 2009. He is working toward the Ph.D. degree at the University of Leuven (KU Leuven), Heverlee, Belgium.

Since 2010, he is a research assistant at KU Leuven. His research interests are the impact of integration of renewable energy sources on the electricity grid and the development of the transmission grid for large-scale renewable integration.

Dirk Van Hertem (S'02–SM'09) was born in 1979, in Neerpelt, Belgium. He received the M.Eng. degree from the KHK, Geel, Belgium, in 2001, and the M.Sc. degree in electrical engineering and the Ph.D. degree from the University of Leuven (KU Leuven), Heverlee, Belgium, in 2003 and 2009, respectively.

In 2010, he became a member of the EPS Group at the Royal Institute of Technology, Stockholm, Sweden, where he was the program manager for controllable power systems for the EKC^2 competence at KTH. Since spring 2011, he is back at KU Leuven where he is an assistant professor in the ELECTA Group. His special fields of interest are power system operation and control in systems with FACTS and HVDC and building the transmission system of the future, including offshore grids and the supergrid concept.

Dr. Van Hertem is an active member of both IEEE (PES and IAS) and Cigré.

Ronnie Belmans (S'77–M'84–SM'89–F'05) received the M.S. degree in electrical engineering and the Ph.D. degree, both from the University of Leuven (KU Leuven), Heverlee, Belgium, in 1979 and 1984, respectively, and the Special Doctorate and the Habilitierung degrees, both from the RWTH, Aachen, Germany, in 1989 and 1993, respectively.

Currently, he is a Full Professor with the KU Leuven, teaching electric power and energy systems. His research interests include techno-economic aspects of power systems, power quality, and distributed generation. He is also Guest Professor at Imperial College of Science, Medicine and Technology, London, U.K.

Dr. Belmans is a Fellow of the Institute of Electrical Engineers (IET, U.K.). He is the Honorary Chairman of the board of Elia, which is the Belgian transmission grid operator. He is also the President of the International Union for Electricity Applications (UIE).